Supporting Information

Bis(diphenylphosphinyl)-functionalized dipyrido-annulated NHC towards copper(I) and silver(I)

Sihan Zhang,[a] Rong Shang,[a] Masaaki Nakamoto,[a] Yohsuke Yamamoto*[a] Yohei Adachi[b] and Joji Ohshita[b]*

[a.] Department of Chemistry, Graduate School of Science, Hiroshima University, Higashi-Hiroshima, 7398526, Japan

[b.] Department of Applied Chemistry, Graduate School of Engineering, Hiroshima University, Higashi-Hiroshima, 7398527, Japan

Table of contents

Kinetic Study of 2 (Ag_2L_2)

A JEOL JNM-ECA 600 NMR spectrometer was used for Variable Temperature (VT)-NMR studies of the solution behaviour of **2** (Ag_2L_2). The probe temperature was calibrated using standard methanol solution purchased from Sigma-Aldrich. The spectra were recorded at set temperatures, the corresponding probe temperatures from calibration curve were used for calculations. The gNMR Spectral Simulation Program (*version 4.1*) was used to simulate the obtained spectra.

From the calibration curve of our instrument, the real probe temperatures were calculated using the calibration equation: $y = -0.0014x^2 + 1.6451x - 63.72$

where x = Set Temperature, y = real probe temperatures.

Table S1. Temperature calibration: correlations between the set and real probe temperatures.

Set Temp /°C	Set Temp /K	Real Probe Temp /°C	Real Probe Temp /K
–65.0	208.2	–55.1	218.1
–70.0	203.2	–60.4	212.8
–75.0	198.2	–65.9	207.3
–80.0	193.2	–71.3	201.9
–85.0	188.2	–76.9	196.3

The hydrogen resonances corresponding to dipyridyl groups of **2** (Ag_2L_2) are shifting depending on the temperature. We plotted chemical shifts against temperatures, and used the best approximation curve to assist the modeling of the chemical shifts (Hz) and half-width (Hz) of the resonances using gNMR. The simulated values for δ1, δ2 (in ppm) and half-widths of signals (in Hz) as well as the rate constant k are listed below (the observed and simulated signals are attached at the end of this section).

Table S2. Simulated parameters from gNMR for an Eyring plot.

Temp. Calibration		gNMR Simulation					Eyring Plot	
Set Temp /°C	**Real Probe Temp /K**	**δ1 / ppm**	**$\nu_{1/2}$ (δ1) /Hz**	**δ2 / ppm**	**$\nu_{1/2}$ (δ2) /Hz**	**k / s^{-1}**	**1/T**	**ln(k/T)**
–65.0	218.1	8.732	48.00	8.720	48.00	205.60	0.00458	–0.06
–70.0	212.8	8.780	12.90	8.704	12.00	54.90	0.00470	–1.35
–75.0	207.3	8.809	25.80	8.695	24.00	10.98	0.00482	–2.94
–80.0	201.9	8.823	19.80	8.698	19.20	1.92	0.00495	–4.66
–85.0	196.3	8.836	12.20	8.708	12.00	0.30	0.00509	–6.48

With the simulated k values at different temperatures, an Eyring plot (ln(*k*/T) *v.s.* 1/T) was created to estimate the ΔG, ΔS and ΔH values according to the equation:

$$\ln(\frac{k}{T}) = -(\frac{\Delta H^{\ddagger}}{R})\frac{1}{T} + (\frac{\Delta S^{\ddagger}}{R}) + \ln(\frac{k_B}{h})$$

where the slope of the plot = $-(\frac{\Delta H^{\ddagger}}{R})$, and the intercept = $(\frac{\Delta S^{\ddagger}}{R}) + \ln(\frac{k_B}{h})$

From the Eyring plot:

Slope = –12705, y-intercept = 58.282

Standard error and standard deviation of intercept: $\sigma_M = 0.958$, $\sigma = 2.143$

Standard error and standard deviation of X variable 1 (1/T): $\sigma_M = 198.238$, $\sigma = 443.274$

$\Delta S^{\ddagger} = 68.60$ cal mol^{-1}K^{-1} = 287.03 J mol^{-1}K^{-1}, $\Delta H^{\ddagger} = 25.30$ kcal mol^{-1} = 105.64 kJ mol^{-1}

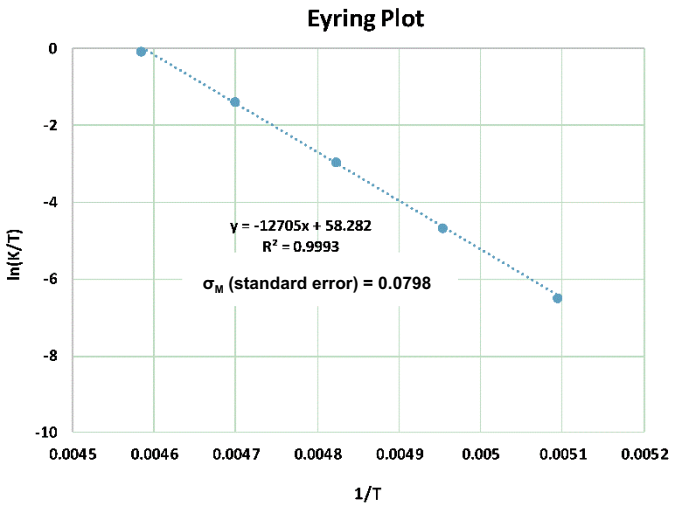

Figure S1. Eyring plot

To verify our simulation, the $\Delta G^{\ddagger}$ value at each temperature was calculated from the obtained ΔS and ΔH values, from which the corresponding k is also calculated according to the rearranged equation:

$$k = (\frac{k_B T}{h})e^{\frac{-\Delta G^{\ddagger}}{RT}}$$

The difference between the calculated k from the Eyring plot and the initial simulated k is within 10%.

Table S3. Calculated and simulated parameters for k at different temperatures.

Set Temp /°C	**Real Probe Temp /K**	**$\Delta G^{\ddagger}$ / kJ mol^{-1}**	**Calculated k** (Eyring plot) /**s^{-1}**	**Simulated k** (gNMR)/**s^{-1}**
–65.0	218.1	43.03	224.72	205.60
–70.0	212.8	44.56	50.73	54.90
–75.0	207.3	46.12	10.39	10.98
–80.0	201.9	47.69	1.91	1.92
–85.0	196.3	49.29	0.31	0.30

gNMR simulation:

Measured NMR Spectra **Simulated Spectra (gNMR)**

–85 **°C**（set temperature） k = 0.30 s^{-1}

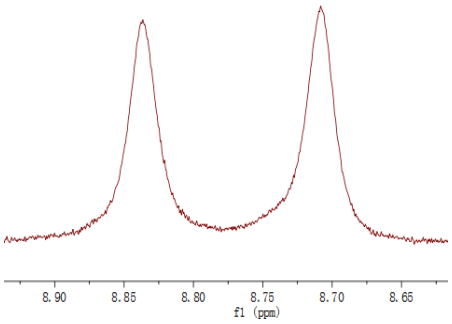

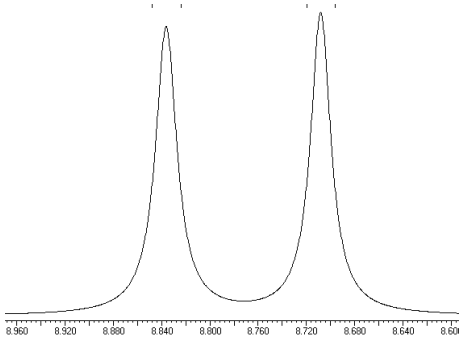

–80 **°C** k = 1.92 s^{-1}

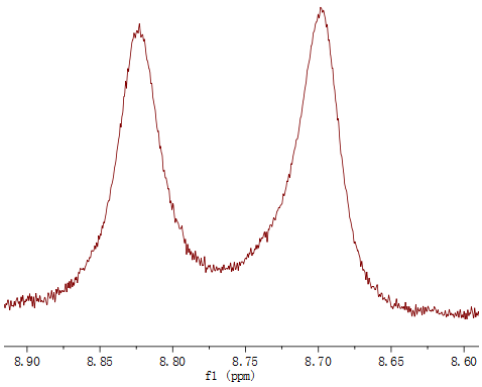

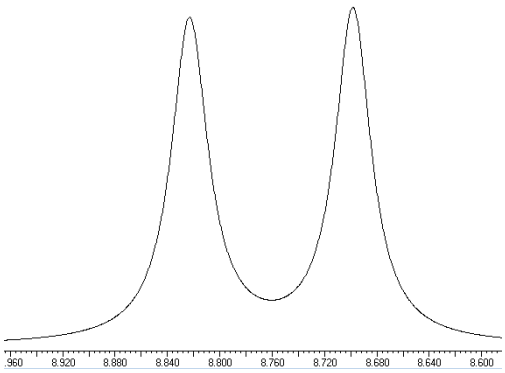

–75 **°C** k = 10.98 s^{-1}

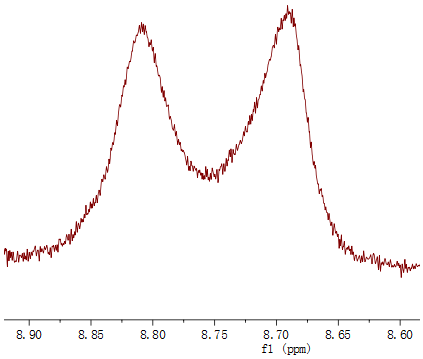

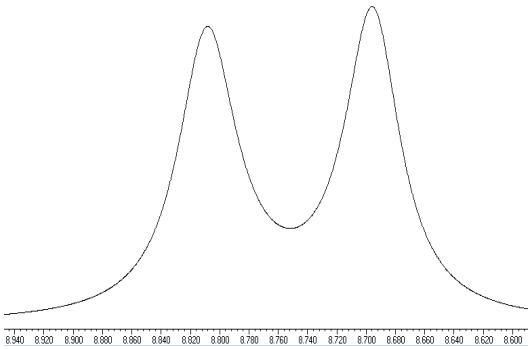

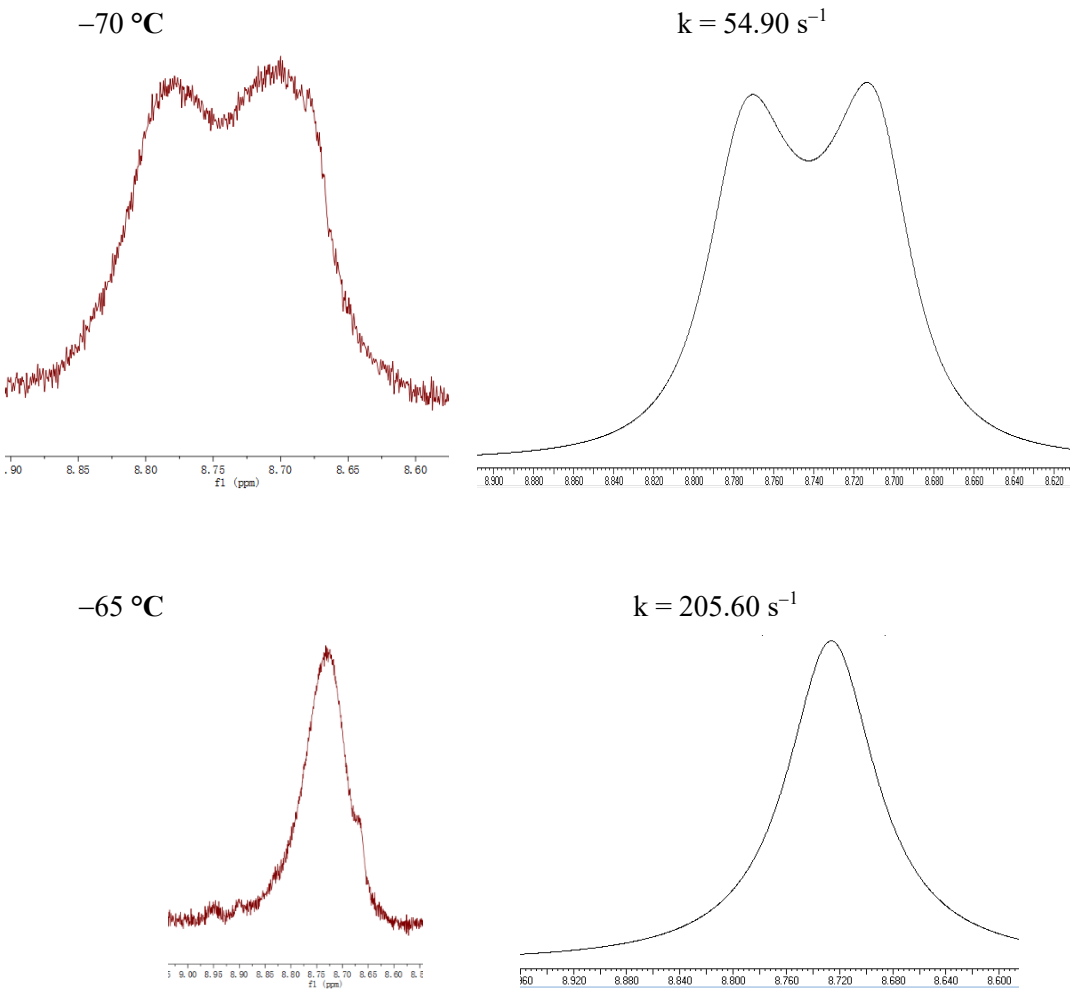

Figure S2. Comparison between measured and simulated spectra

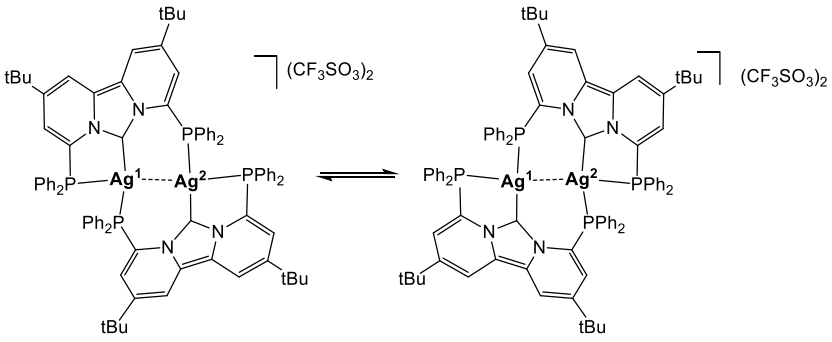

Scheme S1. Proposed fluxional process of dinuclear silver complex **2** (Ag_2L_2) in solution

VT UV-vis absorption spectrum of 3 (Cu_2L_2)

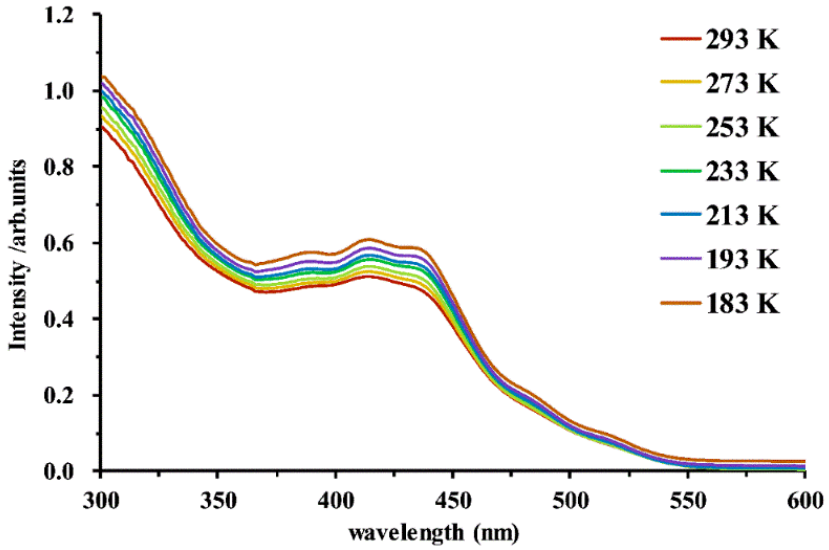

Figure S3. VT UV-vis spectrum of complex **3** (Cu_2L_2) in THF from 293 K to 183 K at concentration of 2.0×10^{-5} M

Photophysical properties

UV-vis absorption spectra were recorded with a Shimadzu UV-1650PC spectrophotometer. Photoluminescence (PL) spectra were measured with a HORIBA FluoroMax-4 spectrophotometer. Preliminary investigation on the photophysical properties of complexes **6** (Cu_4LBr_4), **3** (Cu_2L_2), **4** [$Cu_4L_2(NCMe)_2$], **5** ($Cu_5L_2Br_3$) and **2** (Ag_2L_2) was performed in degassed 2-methyl-THF at room temperature or 77 K.

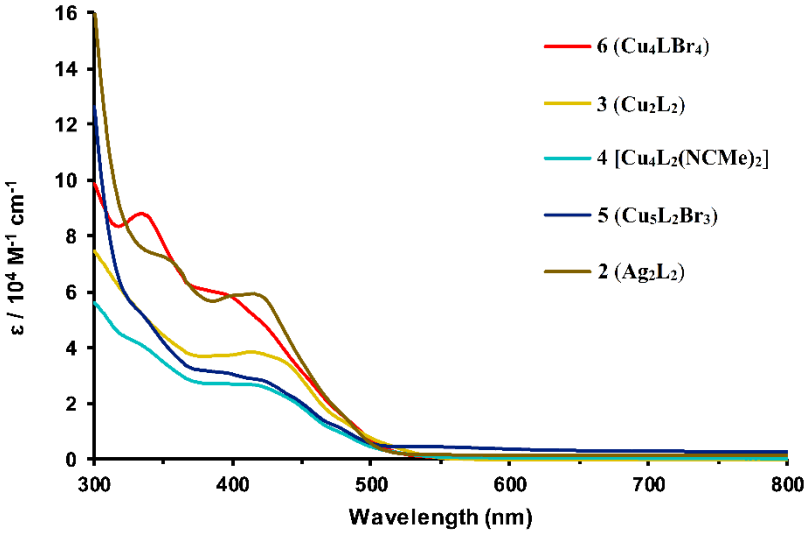

Figure S4. UV-vis absorption spectra of complexes **6** (Cu_4LBr_4), **3** (Cu_2L_2), **4** [$Cu_4L_2(NCMe)_2$], **5** ($Cu_5L_2Br_3$) and **2** (Ag_2L_2) at room temperature in degassed 2-methyl-THF (2×10^{-5} M).

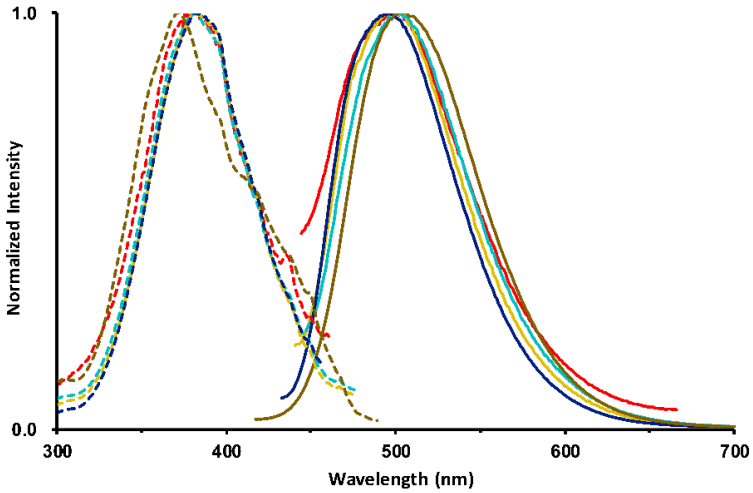

Figure S5. NormalizedExcitation (dashed lines) and emission (solid line) spectra of complexes **6** (Cu_4LBr_4) (red), **3** (Cu_2L_2) (pale yellow), **4** [$Cu_4L_2(NCMe)_2$] (pale blue), **5** ($Cu_5L_2Br_3$) (dark blue) and **2** (**Ag_2L_2**) (dark yellow) at room temperature in degassed 2-methyl-THF (2×10^{-5} M). Samples were excited at 420 nm {**6** (Cu_4LBr_4), **3** (Cu_2L_2), **4** [$Cu_4L_2(NCMe)_2$] and **2** (Ag_2L_2)} and 395 nm [**5** ($Cu_5L_2Br_3$)]. Photoluminescence excitation spectra were recorded by monitoring emissions at 505 nm [**2** (Ag_2L_2)] and 500 nm {**6** (Cu_4LBr_4), **3** (Cu_2L_2), **4** [$Cu_4L_2(NCMe)_2$] and **5** ($Cu_5L_2Br_3$)}.

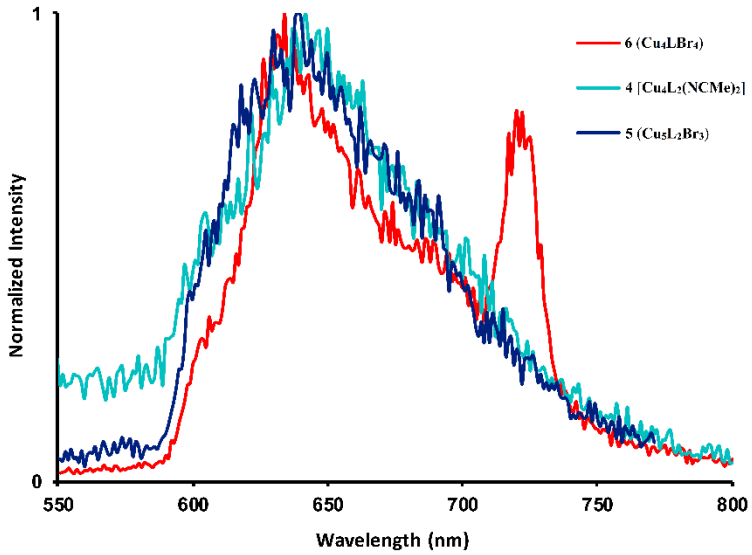

Figure S6. Normalized phosphorescence spectra of **6** (Cu_4LBr_4), **4** [$Cu_4L_2(NCMe)_2$] and **5** ($Cu_5L_2Br_3$) in degassed 2-methyl-THF (2×10^{-5} M) with a delay time of 50 μsec after excitation at 77 K. Samples were excited at 420 nm {**6** (Cu_4LBr_4) and **4** [$Cu_4L_2(NCMe)_2$]} and 395 nm [**5** ($Cu_5L_2Br_3$)].

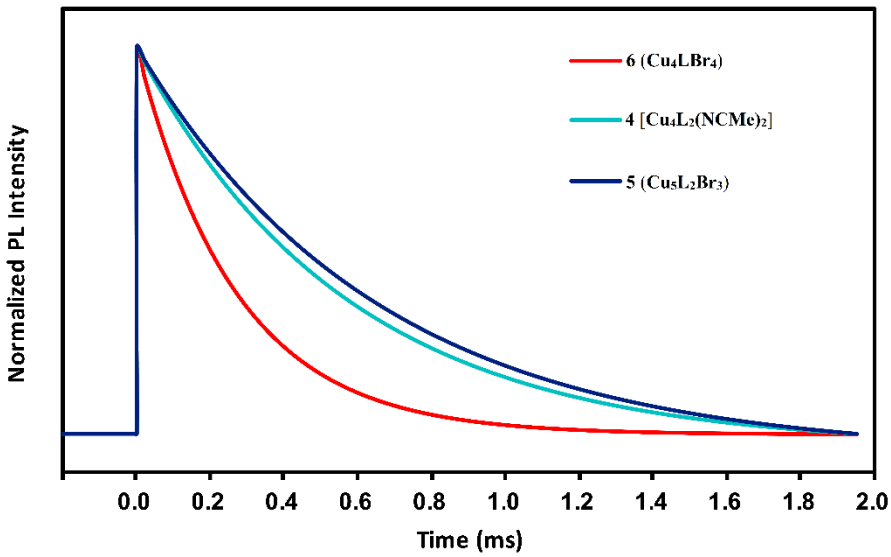

Figure S7. Phosphorescence decay traces for **6** (Cu_4LBr_4), **4** [$Cu_4L_2(NCMe)_2$] and **5** ($Cu_5L_2Br_3$) in degassed 2-methyl-THF (2×10^{-5} M) monitoring at 640 nm at 77 K. The lifetimes of complexes **6** (Cu_4LBr_4), **4** [$Cu_4L_2(NCMe)_2$] and **5** ($Cu_5L_2Br_3$) are 268.7, 571.9 and 655.6 μs, respectively.

Summary of crystal data

Table S4. Crystallographic Data for compounds Ag_2L_2 (2), Cu_2L_2(DMF) (3·DMF), $Cu_5L_2Br_3(DMF)_2$ (5·2DMF) and Cu_4LBr_4 (6).

	Ag_2L_2 (**2**)	Cu_2L_2(DMF) (**3·DMF**)	$Cu_5L_2Br_3(DMF)_2$ (**5·2DMF**)	Cu_4LBr_4 (**6**)
CCDC No.	1920382	1920383	1920384	1920385
formula	$C_{88}H_{84}Ag_2F_6N_4O_6P_4S_2\cdot(CH_3)_2NCHO$	$C_{88}H_{84}Cu_2F_6N_4O_6P_4S_2\cdot(CH_3)_2NCHO\cdot2CH_3CH_2OCH_2CH_3$	$C_{88}H_{84}Br_3Cu_2F_6N_4O_6P_4S_2\cdot2(CH_3)_2NCHO$	$C_{43}H_{42}N_2P_2Br_4Cu_4$
formula weight	1884.42	1906.94	2299.21	1222.57
crystal system	Monoclinic	Monoclinic	Monoclinic	Monoclinic
space group	$P2_1/c$	$P2_1/c$	$P2_1/c$	$P2_1/c$
temperature (K)	123	123	123	123
a (Å)	14.6842(8)	13.0789(17)	29.878(2)	9.3808(6)
b (Å)	28.1889(16)	20.410(3)	13.1902(10)	25.6046(17)
c (Å)	21.6554(12)	34.694(5)	28.148(2)	18.5364(12)
α (˚)	90	90	90	90
β (˚)	106.5630(10)	92.526(2)	117.0600(10)	97.0900(10)
γ (˚)	90	90	90	90
V (Å^3)	8591.9(8)	9252(2)	9878.7(13)	4418.2(5)
Z	4	4	4	2
d_{calcd} (g cm^{-3})	1.457	1.369	1.546	1.838
μ (mm^{-1})	0.650	0.645	2.447	5.622
F_{000}	3872	3980	4656	2400
no. reflns	45485	48648	51294	23849
no. unique reflns	17532	18706	20103	9337
R_{int}	0.0282	0.0573	0.0393	0.1118
R_1 [$I > 2\,\sigma\,(I)$]	0.0441	0.0444	0.0795	0.0558
wR_2 (all data)	0.1233	0.1242	0.2276	0.1696
GOF	1.025	1.021	1.093	1.026

NMR spectra

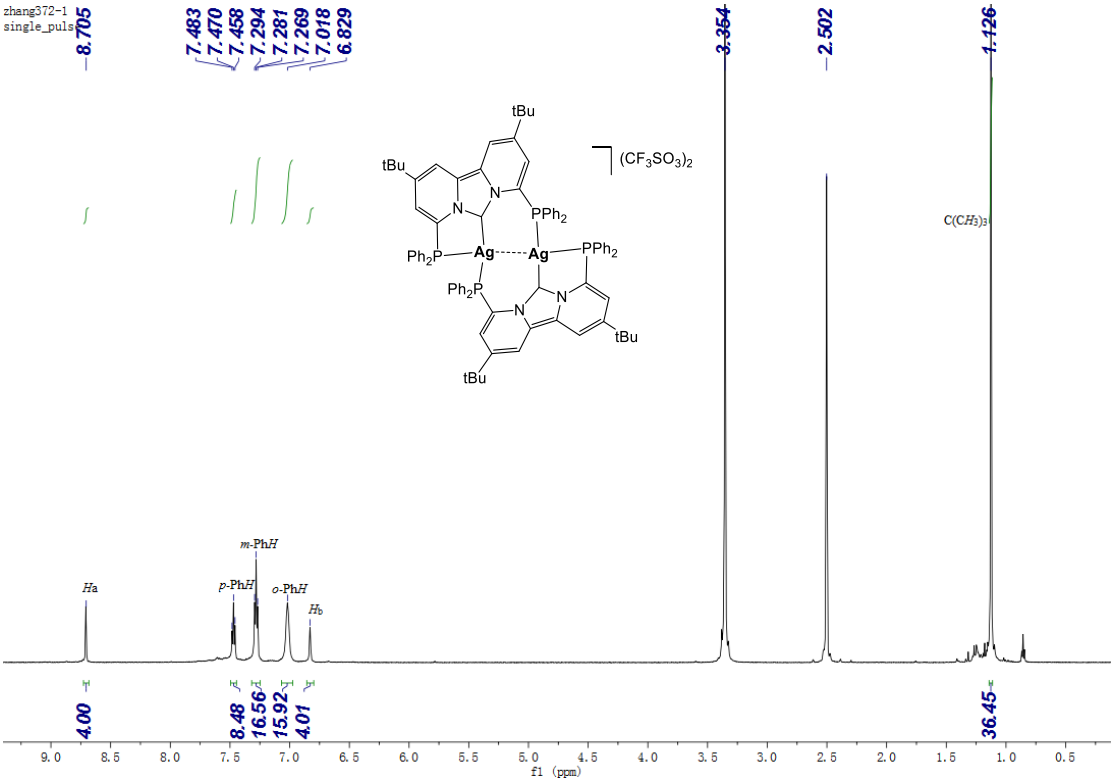

Figure S8. ^{1}H NMR spectrum (600 MHz) of **2** (Ag_2L_2) in DMSO-d_6

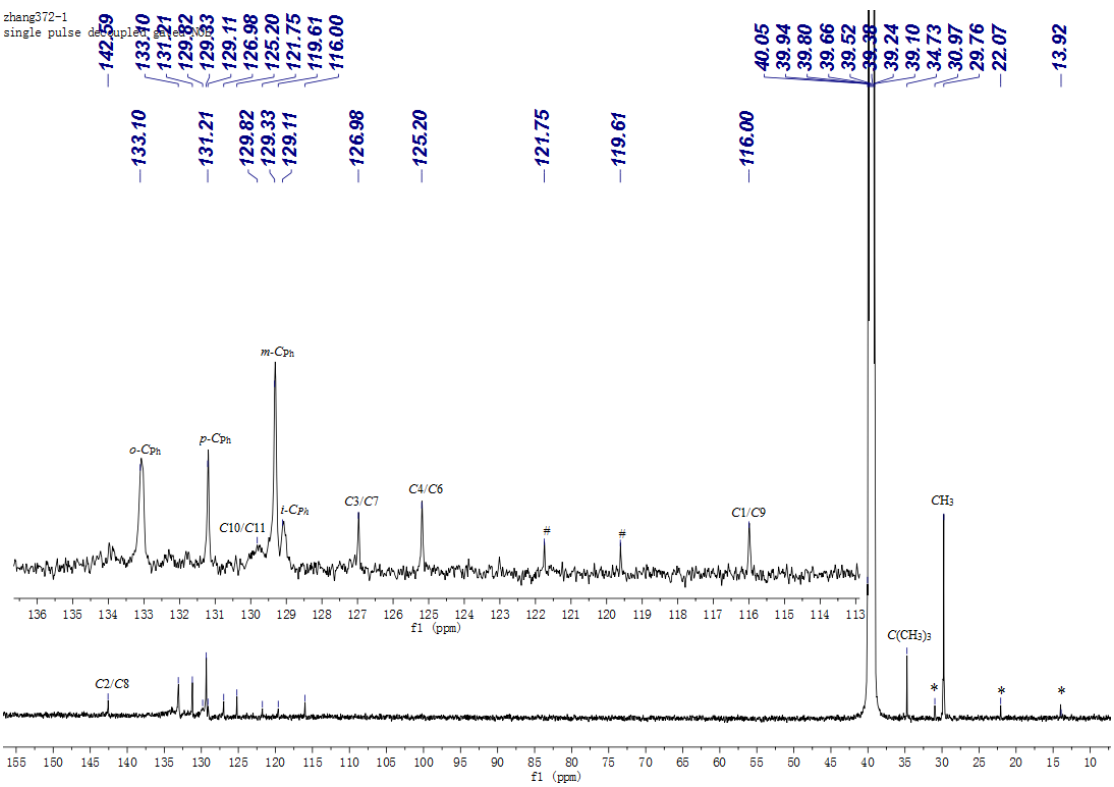

Figure S9. ^{13}C{^{1}H} NMR spectrum (150 MHz) of **2** (Ag_2L_2) in DMSO-d_6 (# = CF_3, * = hexane)

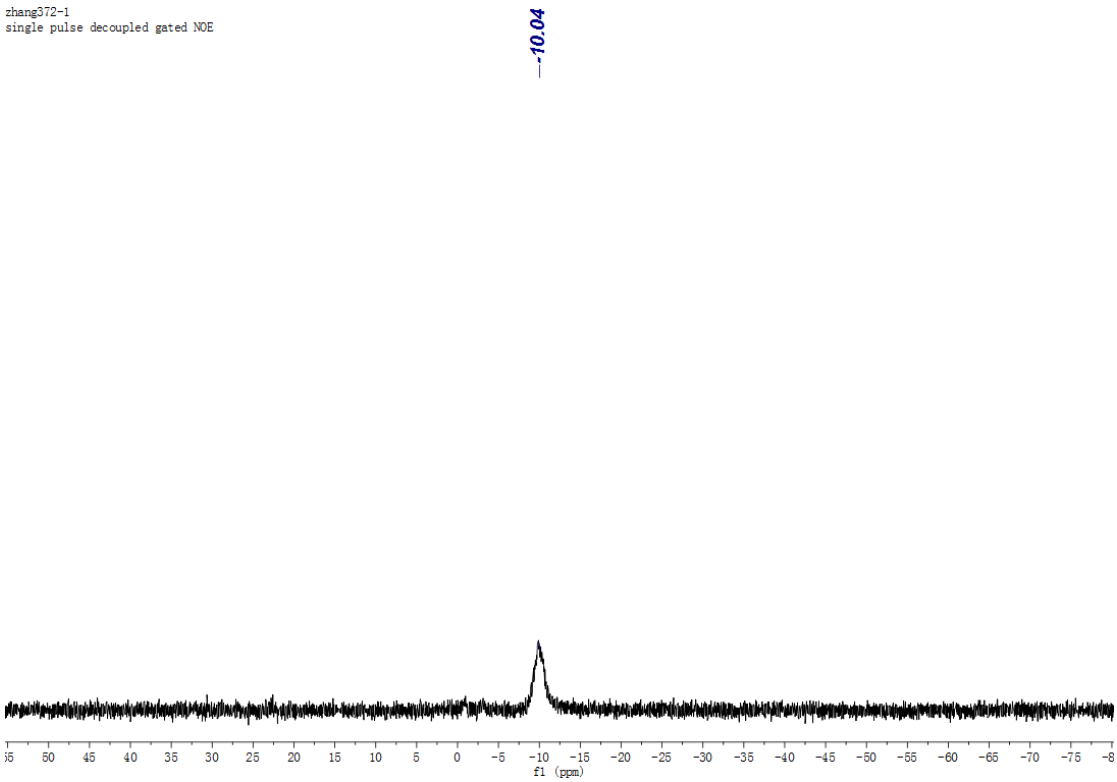

Figure S10. $^{31}P\{^{1}H\}$ NMR spectrum (243 MHz) of **2** (Ag_2L_2) in DMSO-d_6 at 293 K.

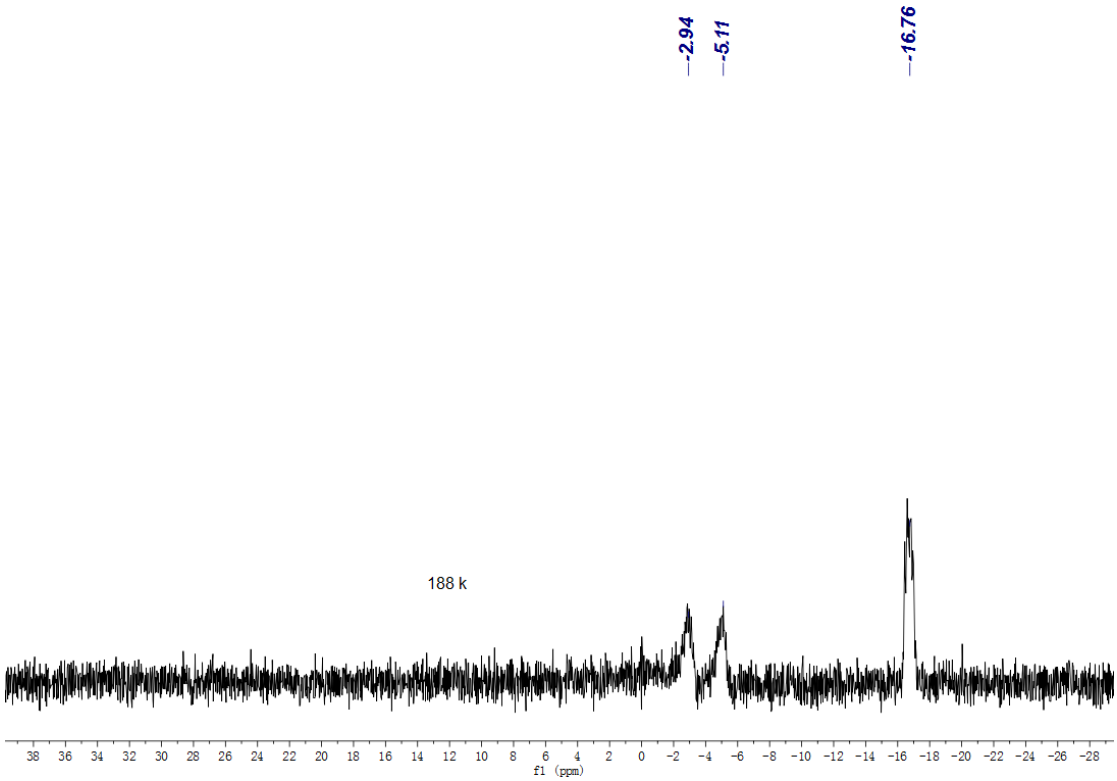

Figure S11. $^{31}P\{^{1}H\}$ NMR spectrum (243 MHz) of **2** (Ag_2L_2) in THF-d_8 at 188 K

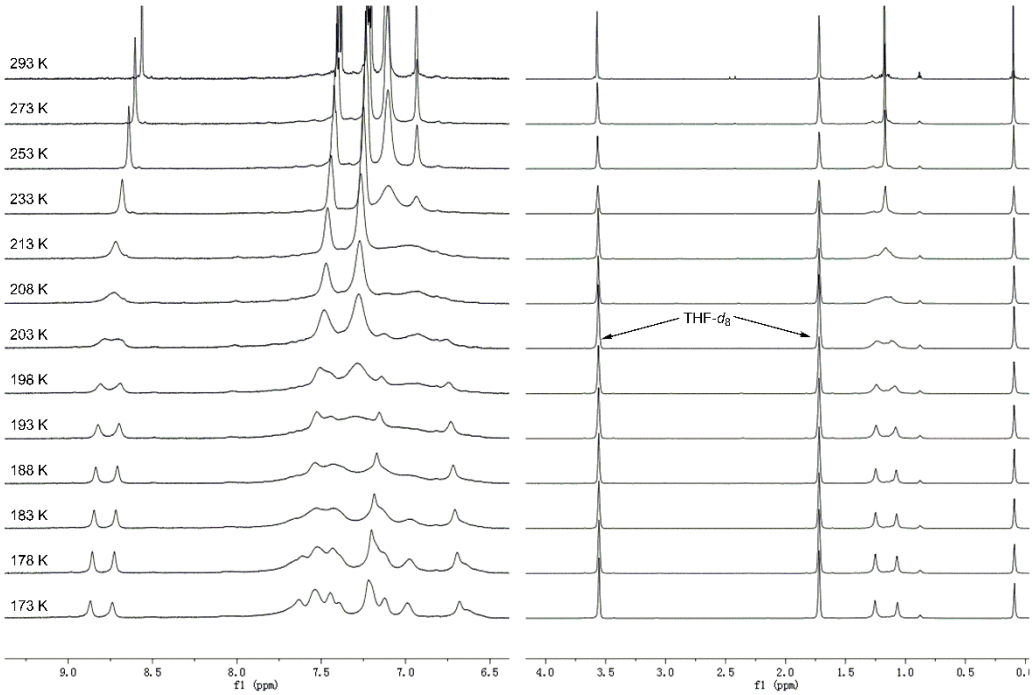

Figure S12. VT ^{1}H NMR spectrum (600 MHz) of **2** (Ag_2L_2) in THF-d_8 from 293 K to 173 K.

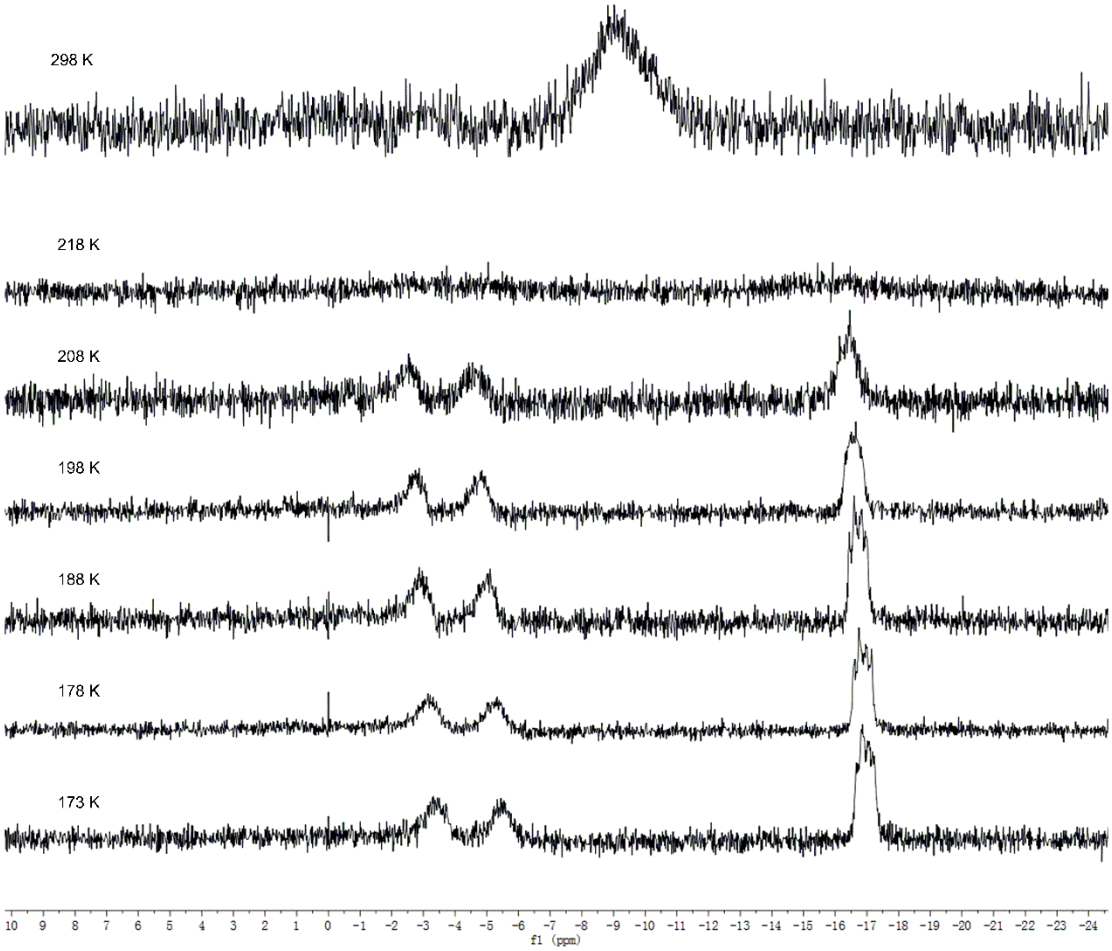

Figure S13. VT $^{31}P\{^{1}H\}$ NMR spectrum (243 MHz) of **2** (Ag_2L_2) in THF-d_8 from 293 K to 173 K.

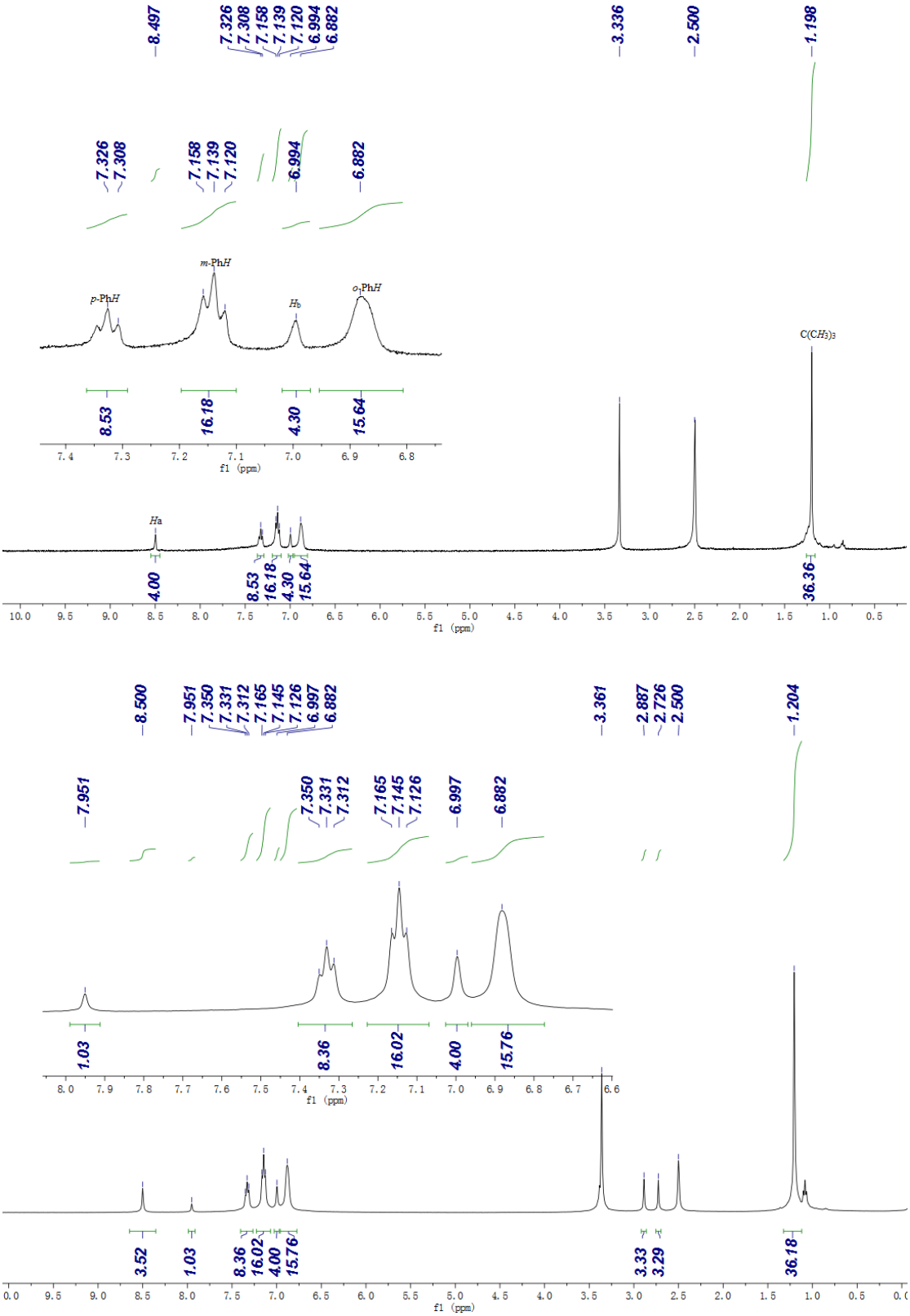

Figure S14. ^{1}H NMR spectrum (600 MHz) of **3** (Cu_2L_2) (bulk sample) in DMSO-d_6 (top); ^{1}H NMR spectrum (600 MHz) of **3·DMF** [Cu_2L_2(DMF)] (crystals) in DMSO-d_6 (singlets at 7.95, 2.89 and 2.73 ppm for the coordinated DMF) (bottom)

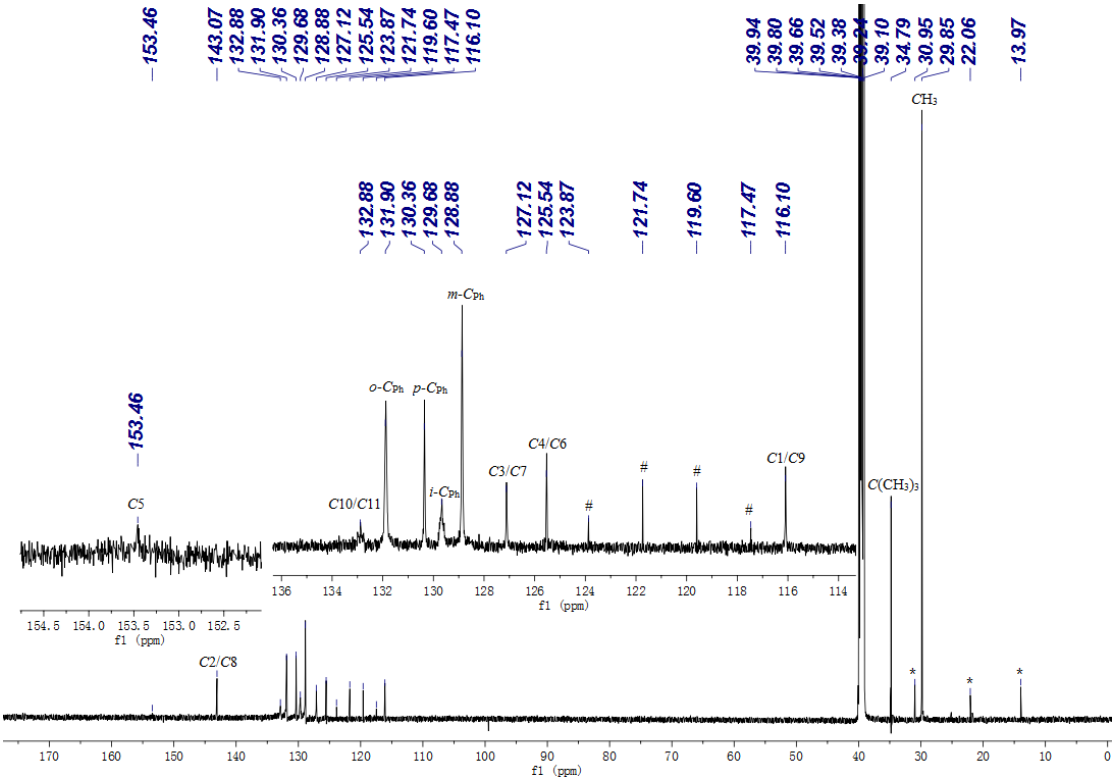

Figure S15. $^{13}C\{^{1}H\}$ NMR spectrum (150 MHz) of **3** (Cu_2L_2) (bulk sample) in DMSO-d_6 (# = CF_3, * = hexane)

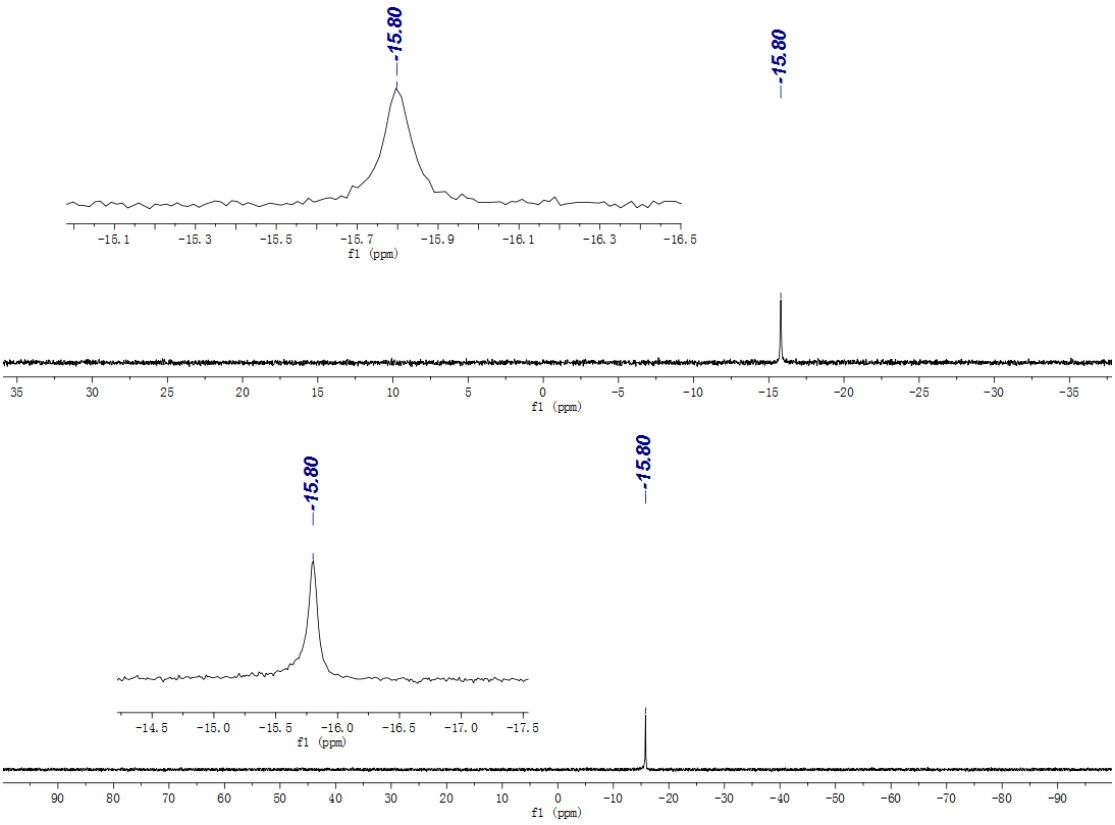

Figure S16. $^{31}P\{^{1}H\}$ NMR spectrum (243 MHz) of **3** (Cu_2L_2) (bulk sample) in DMSO-d_6 (top); $^{31}P\{^{1}H\}$ NMR spectrum (243 MHz) of **3·DMF** [Cu_2L_2(DMF)] (crystals) in DMSO-d_6 (bottom)

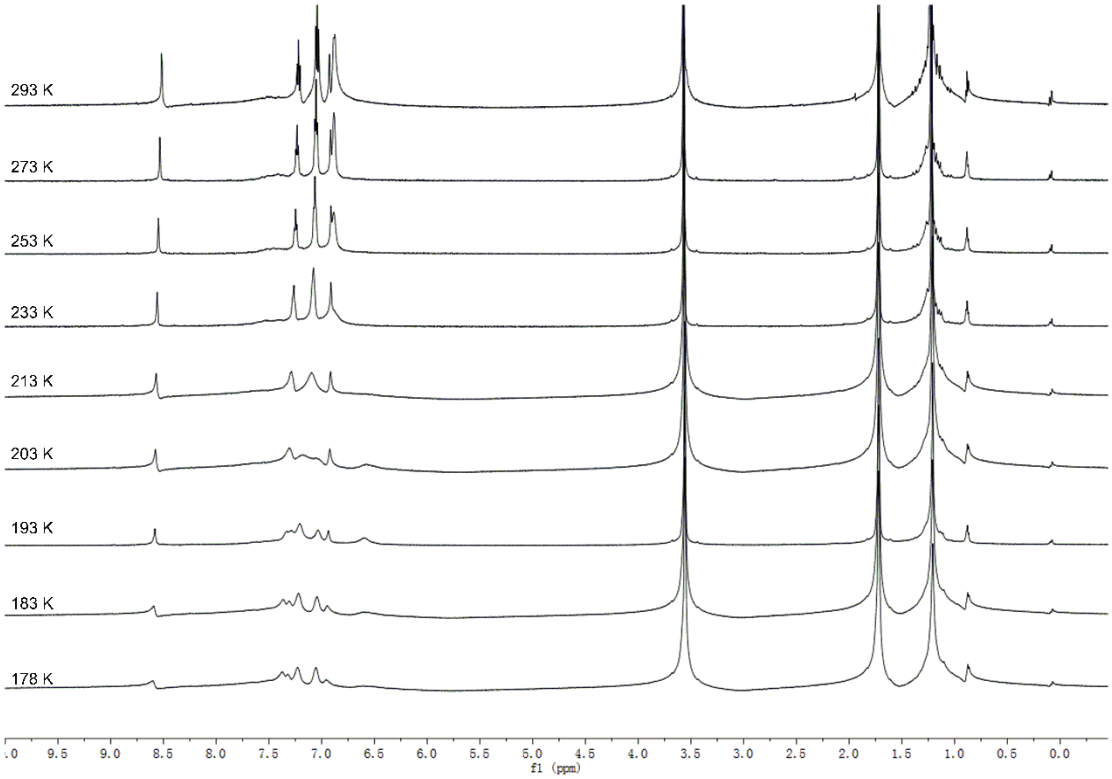

Figure S17. VT ^{1}H NMR spectrum (600 MHz) of **3** (Cu_2L_2) in THF-d_8

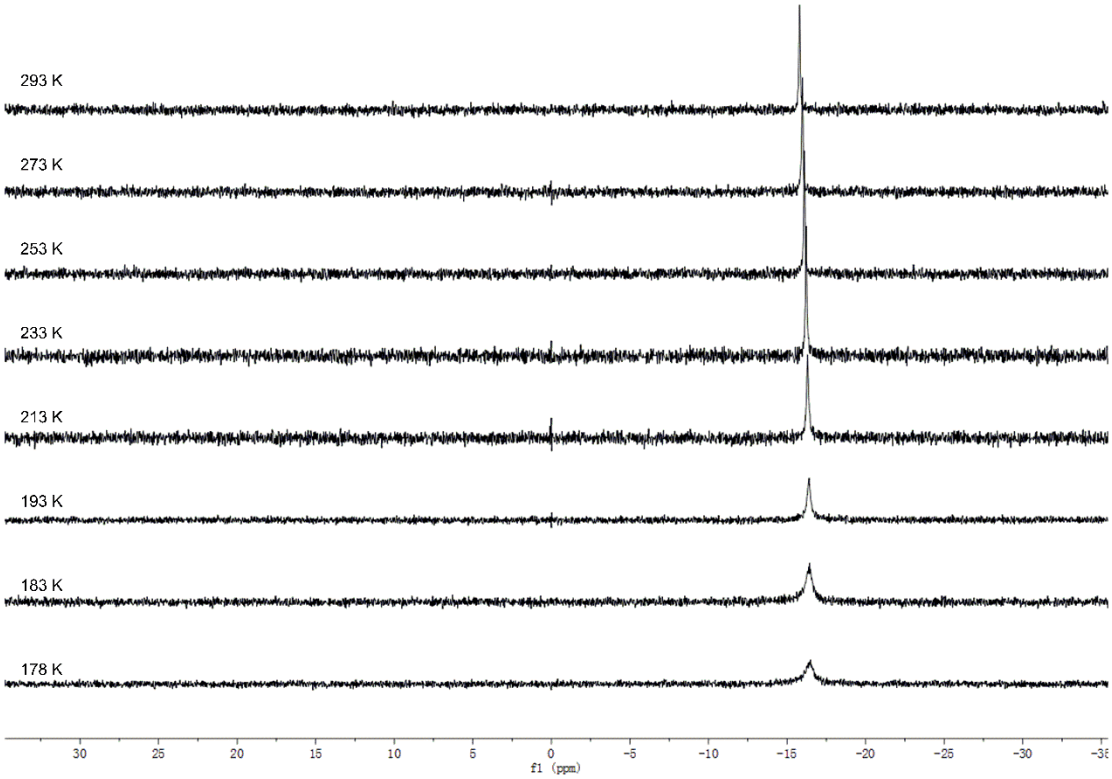

Figure S18. VT ^{31}P NMR spectrum (600 MHz) of **3** (Cu_2L_2) in THF-d_8 from 293 K to 178 K.

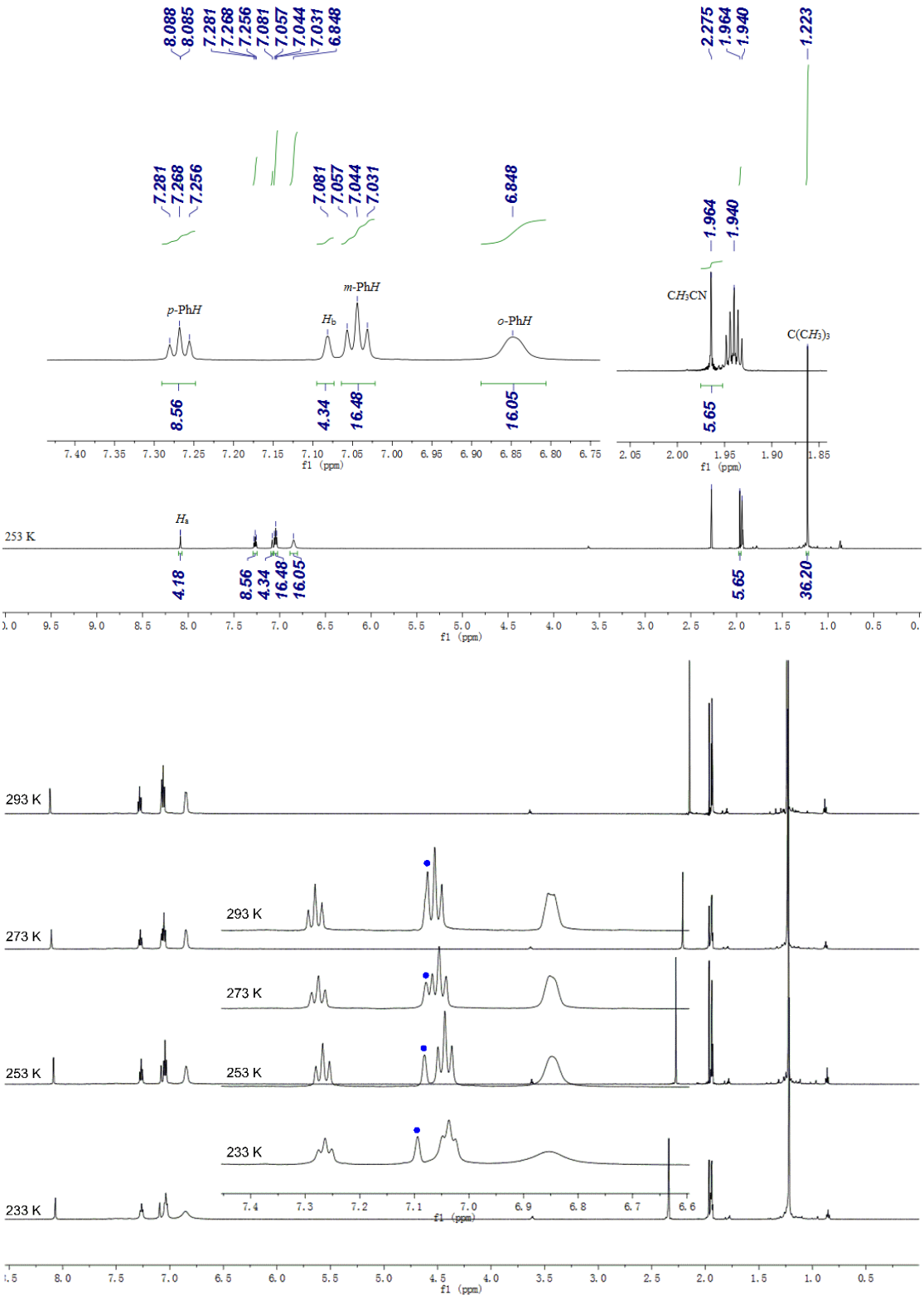

Figure S19. ^{1}H NMR spectra (600 MHz) at 253 K (top) and VT ^{1}H NMR spectrum from 293 to 233 K (bottom) of **4** $[Cu_4L_2(NCMe)_2]$ in CD_3CN

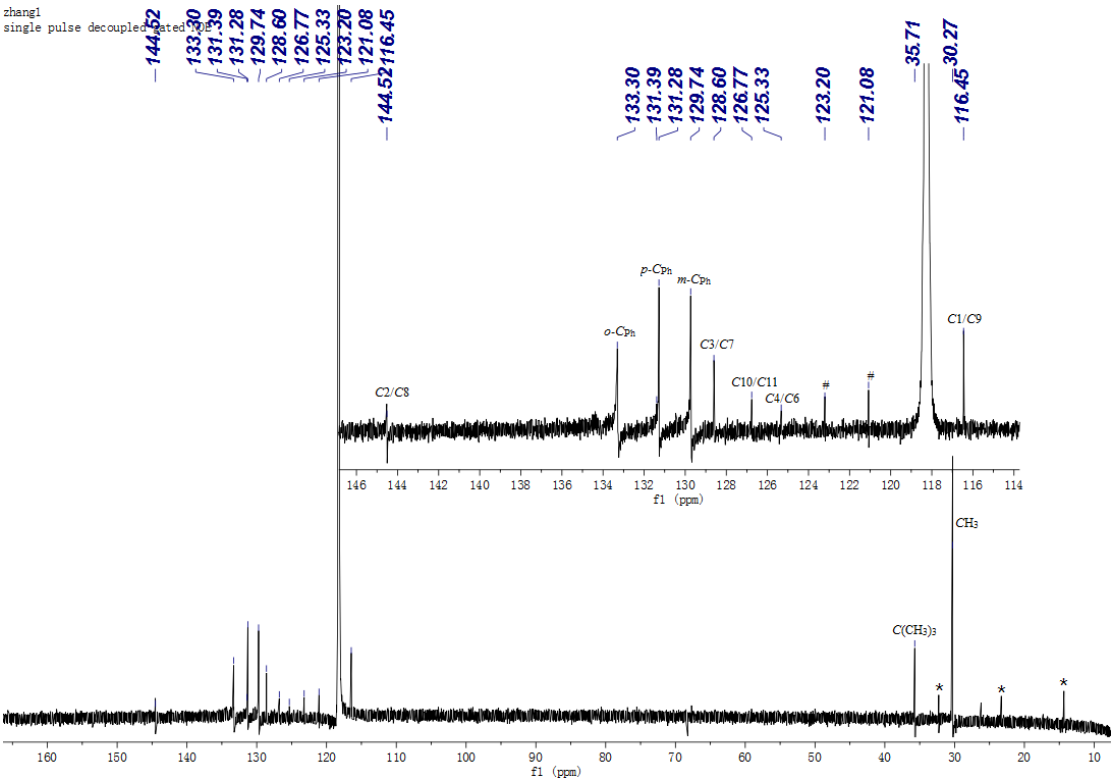

Figure S20. $^{13}C\{^{1}H\}$ NMR spectrum (150 MHz) of **4** $[Cu_4L_2(NCMe)_2]$ in CD_3CN (# = CF_3, * = hexane)

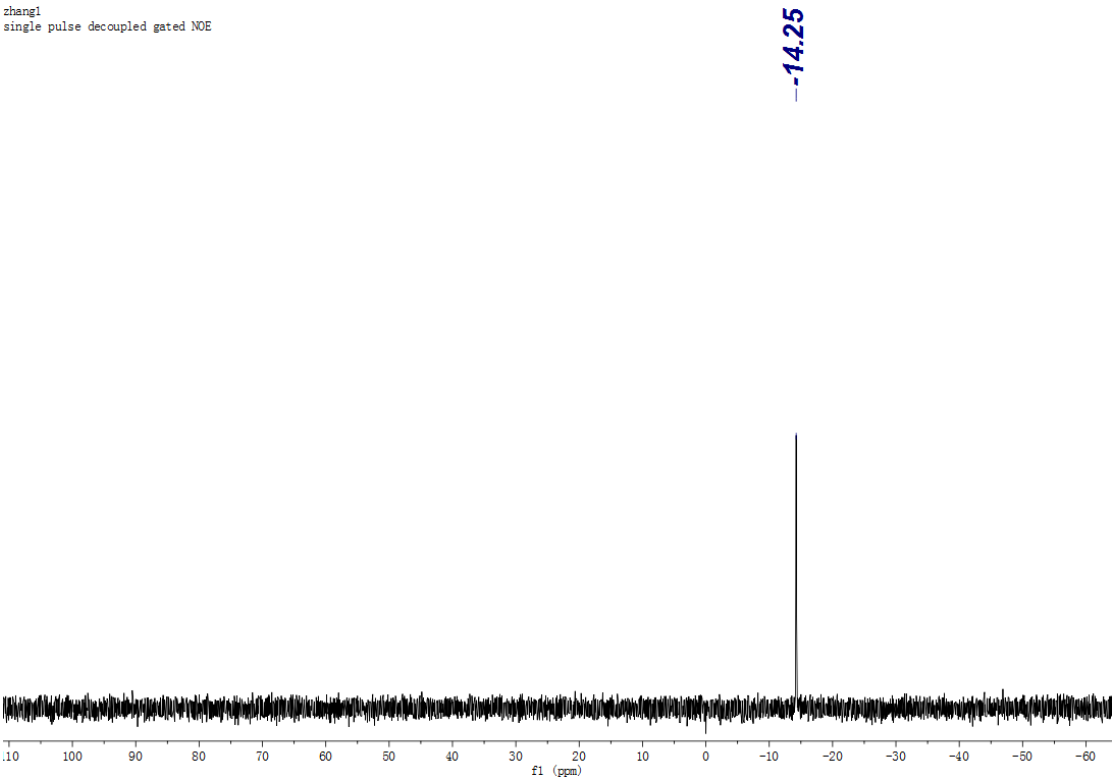

Figure S21. $^{31}P\{^{1}H\}$ NMR spectrum (243 MHz) of **4** $[Cu_4L_2(NCMe)_2]$ in CD_3CN

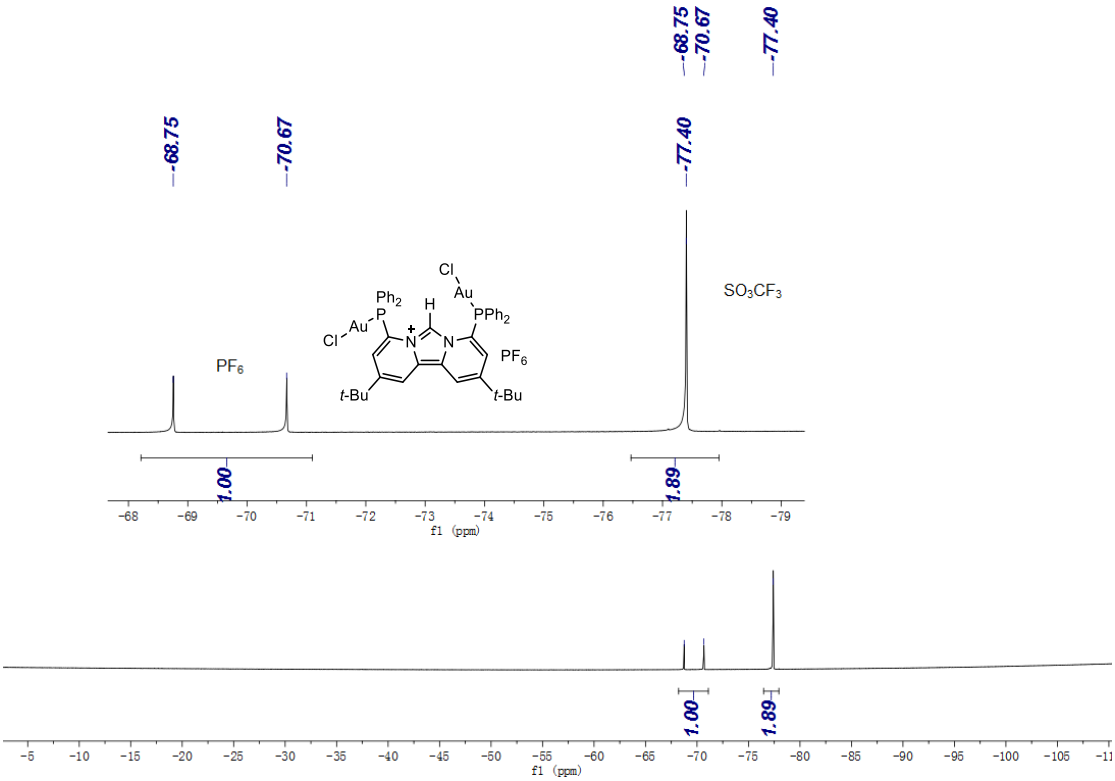

Figure S22. ^{19}F NMR spectrum (376 MHz) of the mixture of equimolar amount of **4** [$Cu_4L_2(NCMe)_2$] and **Au_2Cl_2(dpa^{P2}-NHC)H(PF_6)**[1] in DMSO-d_6

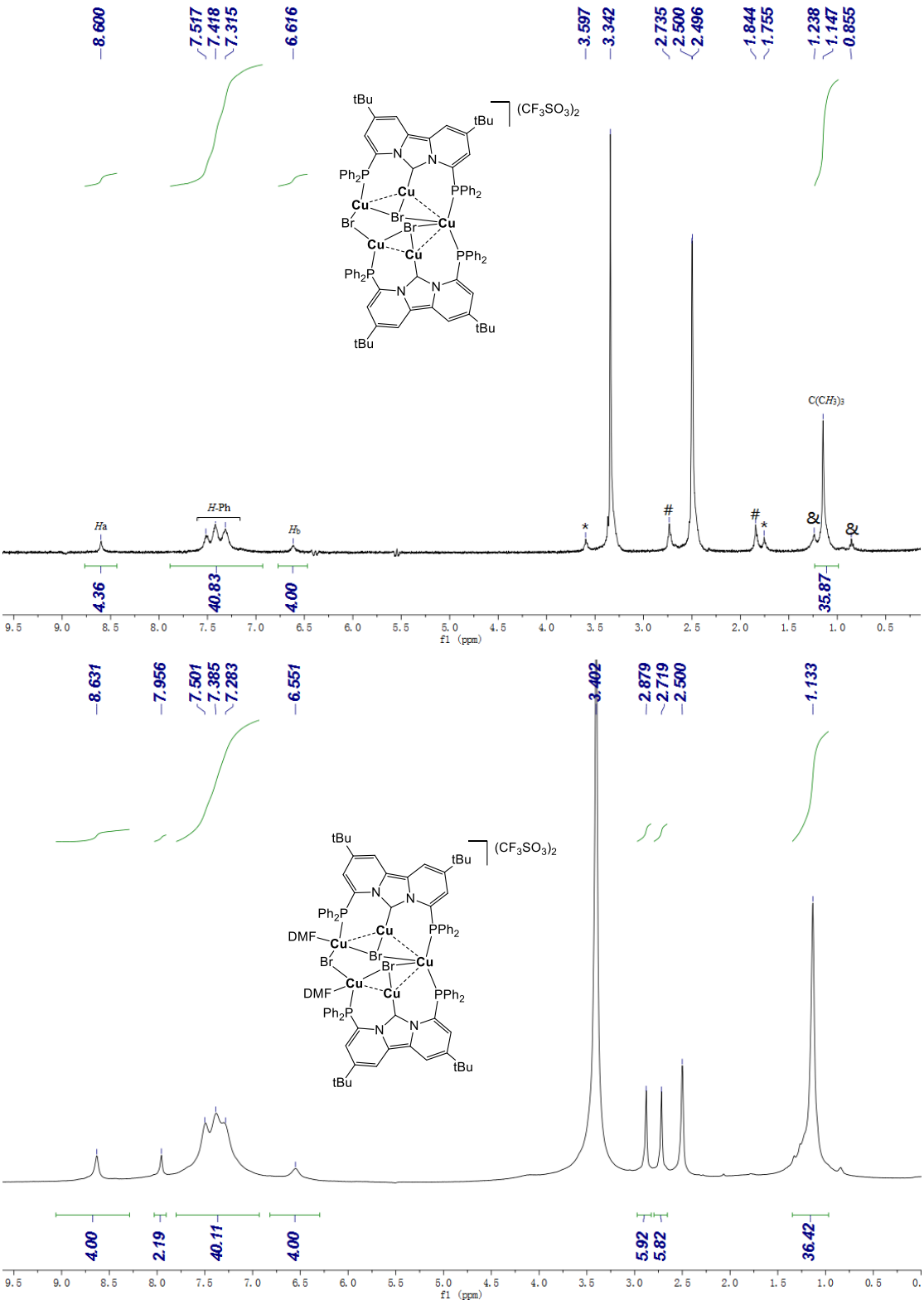

Figure S23. ^{1}H NMR spectrum (600 MHz) of **5** ($Cu_5L_2Br_3$) (bulk sample) in DMSO-d_6 (* = THF, # = tht, & = hexane) (top); ^{1}H NMR spectrum (600 MHz) of **5·2DMF** [$Cu_5L_2Br_3(DMF)_2$] (crystals) in DMSO-d_6 (bottom) (singlets at 7.96, 2.88, 2.72 ppm for DMF);

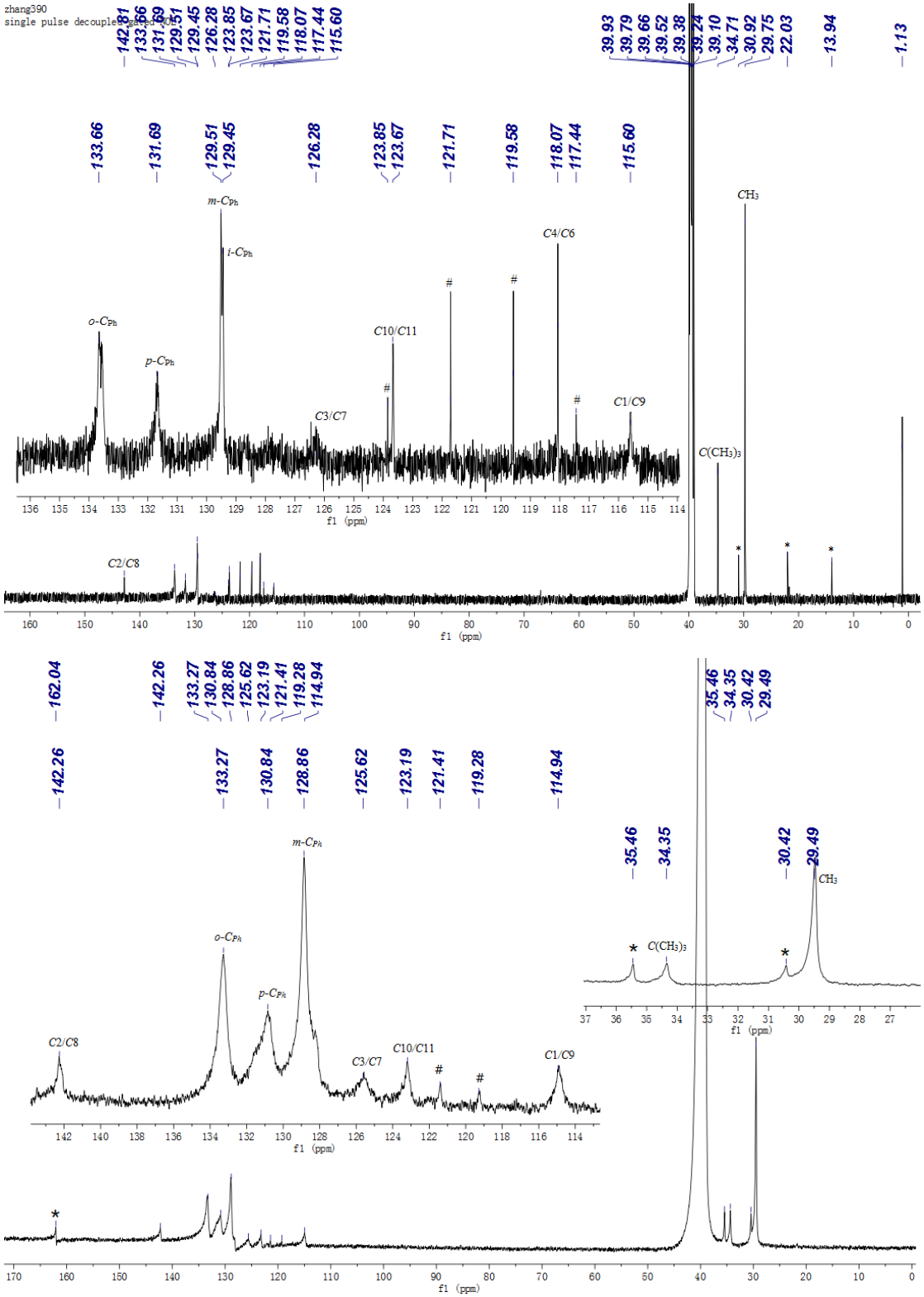

Figure S24. $^{13}C\{^{1}H\}$ NMR spectrum (150 MHz) of **5** ($Cu_5L_2Br_3$) (bulk sample) in DMSO-d_6 (# = CF_3, * = hexane) (top); $^{13}C\{^{1}H\}$ NMR spectrum (150 MHz) of **5·2DMF** [$Cu_5L_2Br_3(DMF)_2$] (crystals) in DMSO-d_6 (# = CF_3, * = DMF) (bottom).

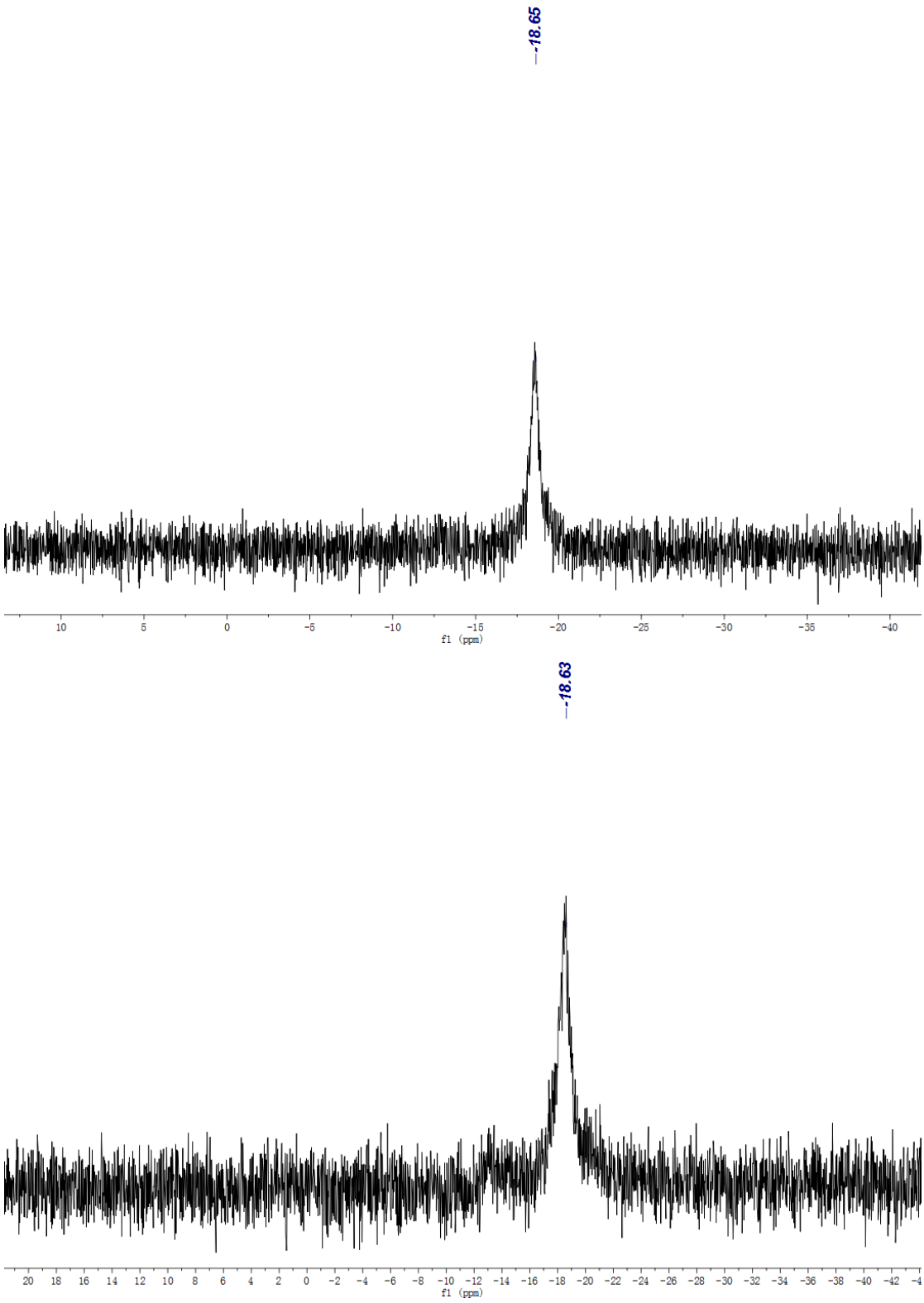

Figure S25. $^{31}P\{^{1}H\}$ NMR spectrum (243 MHz) of **5** ($Cu_5L_2Br_3$) (bulk sample) in DMSO-d_6; $^{31}P\{^{1}H\}$ NMR spectrum (243 MHz) of **5·2DMF** [$Cu_5L_2Br_3(DMF)_2$] (crystals) in DMSO-d_6 (bottom)

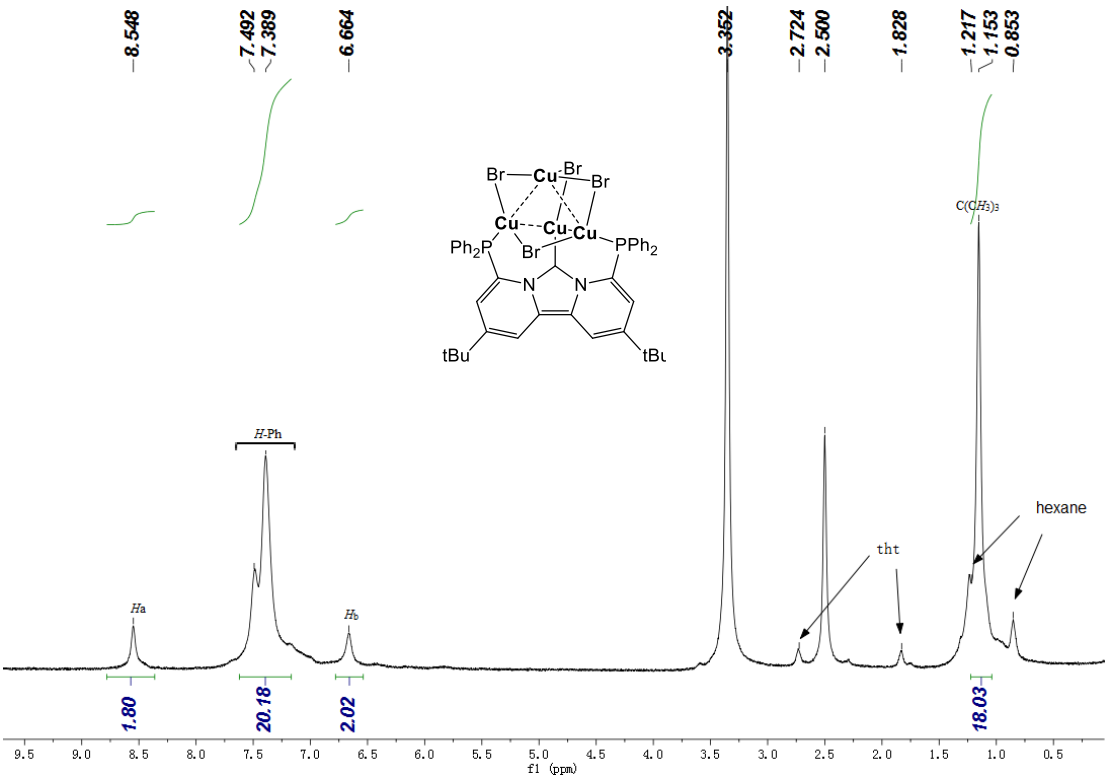

Figure S26. ^{1}H NMR spectrum (400 MHz) of **6** (Cu_4LBr_4) in DMSO-d_6

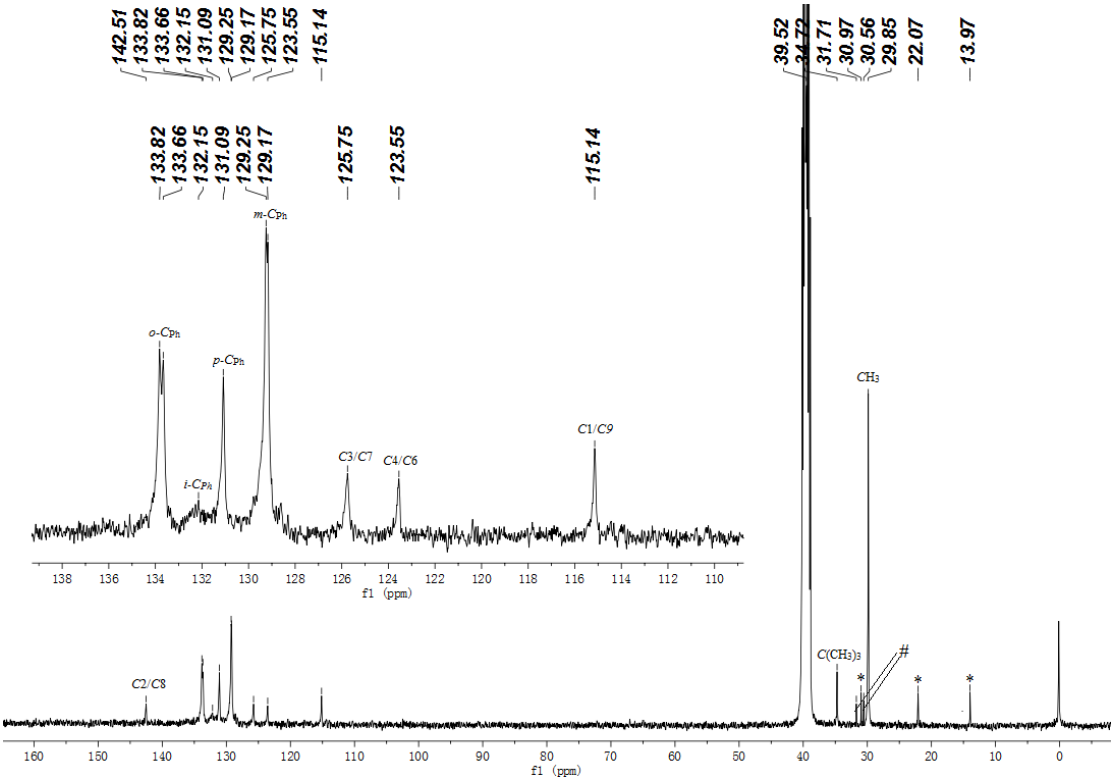

Figure S27. ^{13}C{^{1}H} NMR spectrum (100 MHz) of **6** (Cu_4LBr_4) in DMSO-d_6 (* = hexane, # = tht)

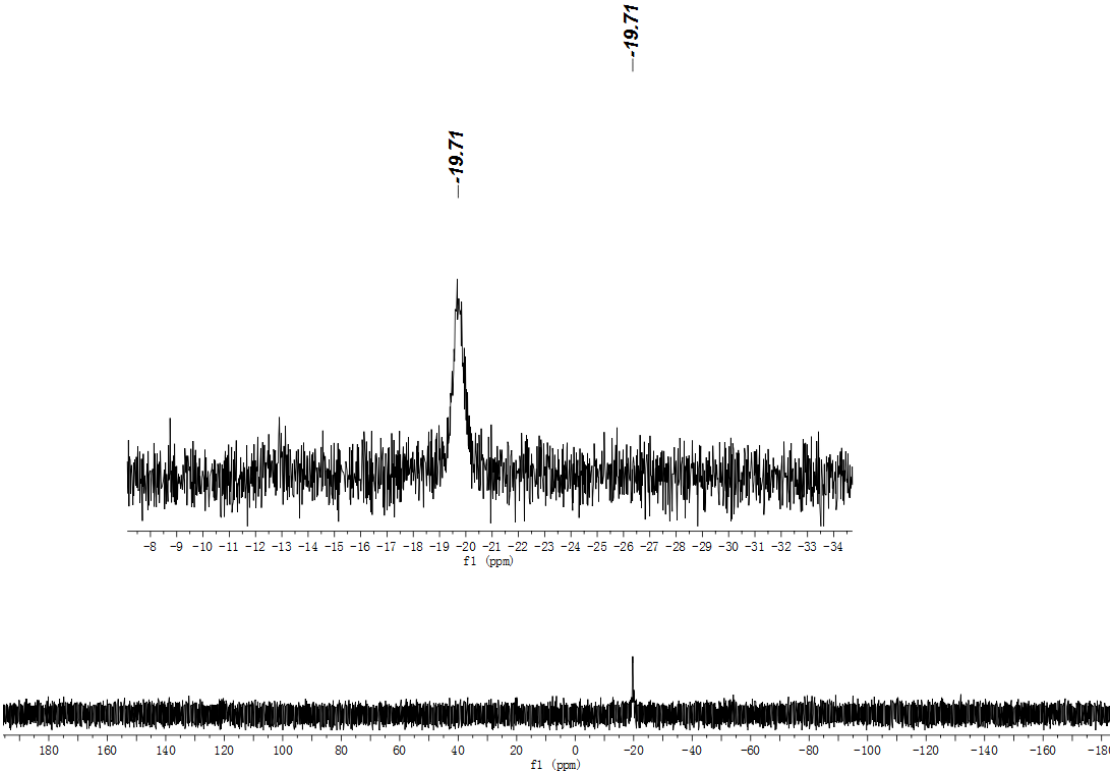

Figure S28. $^{31}P\{^{1}H\}$ NMR spectrum (162 MHz) of **6** (Cu_4LBr_4) in DMSO-d_6

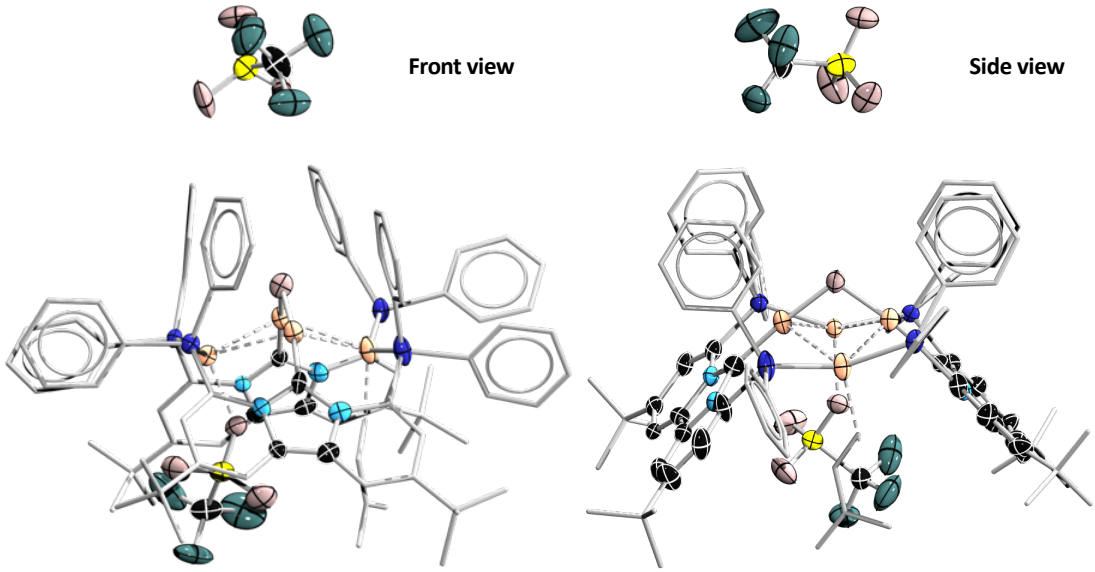

Figure S29. Solid-state structures of the oxygenated species from recrystallisation of **4**. Thermal ellipsoids are set at 50% probability. Ellipsoids of periphery atoms are omitted for clarity. Data is not publishable.

Reference

1. S. Zhang, R. Shang, M. Nakamoto, Y. Yamamoto, Y. Adachi, J. Ohshita, *Inorg. Chem.*, **2019**, 58, 6328-6335.